OPEN ACCESS
CellPress

Cell Reports
Article

A Comprehensive and High-Resolution Genome-wide Response of p53 to Stress

Gue Su Chang,[1,2,3] Xiangyun Amy Chen,[1,2] Bongsoo Park,[1,2] Ho Sung Rhee,[1,2,4] Pingxin Li,[1,2,5] Kang Hoo Han,[1,2] Tejaswini Mishra,[1,2] Ka Yim Chan-Salis,[1,2] Yunfei Li,[1,2,6] Ross C. Hardison,[1,2] Yanming Wang,[1,2] and B. Franklin Pugh[1,2,*]

[1]Center for Eukaryotic Gene Regulation, Department of Biochemistry and Molecular Biology, The Pennsylvania State University, University Park, PA 16802, USA

[2]Center for Comparative Genomics and Bioinformatics, Department of Biochemistry and Molecular Biology, The Pennsylvania State University, University Park, PA 16802, USA

[3]Present address: The Genome Institute, Washington University, School of Medicine, St. Louis, MO 63108, USA

[4]Present address: Departments of Pathology and Cell Biology, Neurology and Neuroscience, Center for Motor Neuron Biology and Disease, Columbia University Medical Center, New York, NY 10032, USA

[5]Present address: 5380 Shamrock Common, Fremont, CA 94555, USA

[6]Present address: Life Technologies, 200 Oyster Point Boulevard, South San Francisco, CA 94080, USA

*Correspondence: bfp2@psu.edu

http://dx.doi.org/10.1016/j.celrep.2014.06.030

SUMMARY

Tumor suppressor p53 regulates transcription of stress-response genes. Many p53 targets remain undiscovered because of uncertainty as to where p53 binds in the genome and the fact that few genes reside near p53-bound recognition elements (REs). Using chromatin immunoprecipitation followed by exonuclease treatment (ChIP-exo), we associated p53 with 2,183 unsplit REs. REs were positionally constrained with other REs and other regulatory elements, which may reflect structurally organized p53 interactions. Surprisingly, stress resulted in increased occupancy of transcription factor IIB (TFIIB) and RNA polymerase (Pol) II near REs, which was reduced when p53 was present. A subset associated with antisense RNA near stress-response genes. The combination of high-confidence locations for p53/REs, TFIIB/Pol II, and their changes in response to stress allowed us to identify 151 high-confidence p53-regulated genes, substantially increasing the number of p53 targets. These genes composed a large portion of a predefined DNA-damage stress-response network. Thus, p53 plays a comprehensive role in regulating the stress-response network, including regulating noncoding transcription.

INTRODUCTION

p53, the "guardian" of the genome, is a sequence-specific transcription factor that, along with other factors, regulates genes involved in stress responses such as UV-induced DNA damage (Menendez et al., 2009; Ptashne and Gann, 1997; Riley et al., 2008). p53 is one of the most commonly mutated proteins in cancers (Donehower and Bradley, 1993). Knowing exactly where p53 binds across a genome, which genes it regulates and how, has been a critical limitation in defining p53's protective functions. Indeed, the current set of p53 targets does not fully explain p53's protective effects (Ma, 2011). Dysfunction of p53 has largely been attributed to defects in p53's DNA binding surface (Freed-Pastor and Prives, 2012; Vogelstein and Kinzler, 1992). However, mutations in a p53 recognition element (RE) could also impair p53's ability to regulate its target gene (Bandele et al., 2011; Naqvi et al., 2010), and this has been largely refractory to study due to the uncertainty of precisely where p53 binds in a genome.

Thousands of putative p53-bound locations have been reported across the human genome (Botcheva et al., 2011; Cawley et al., 2004; Menendez et al., 2013; Nikulenkov et al., 2012; Schlereth et al., 2013; Smeenk et al., 2011; Smeenk et al., 2008; Wang et al., 2014; Wei et al., 2006; Yu et al., 1999; Zhao et al., 2000). However, confidence in such locations is limited by assay sensitivity (signal:noise) that tends to detect the most highly occupied regions and assay resolution having positional uncertainty of several hundred base pairs rather than pinpointing its exact location. Importantly, current RE descriptions lack sufficient uniqueness to confidently identify all but the most robust REs. For example, a recent chromatin immunoprecipitation sequencing (ChIP-seq) study predicted an RE in only half of all 743 high-confidence p53 ChIP-seq peaks (Botcheva et al., 2011).

A p53 RE is comprised of two 10 bp half-sites that have the highly degenerate consensus sequence $(RRRCWWGYYY)_2$, where RWY = A/G, A/T, and C/T, respectively. However, deviations from this consensus are common, and REs reportedly tolerate 1–13 bp insertions between each half-site, deletion of half-sites, and RRRCW quarter sites in multiple orientations (el-Deiry et al., 1992; Funk et al., 1992; Riley et al., 2008). These criteria, if correct, allow for many millions of potential REs across a genome. Because p53 binding may be enriched in

nucleosomal regions (Lidor Nili et al., 2010), invoking chromatin occlusion of REs does not provide an adequate explanation as to the restriction of p53 binding to only a small fraction of putative sites. Thus, a comprehensive, as opposed to statistically enriched, genome-wide identification of p53-bound REs has not yet been achieved.

A general paradigm is that p53 mainly regulates protein-coding genes as both a local core promoter factor and as part of a long-distance enhancer (Riley et al., 2008; Thut et al., 1995). The notion of an enhancer being far from the gene (or transcription unit) that it regulates has been clouded by the discovery of enhancer RNAs (eRNAs), which are produced near enhancers (Kim et al., 2010; Ørom and Shiekhattar, 2013). Although eRNAs tend to be nonpolyadenylated, capped and polyadenylated forms also exist (Djebali et al., 2012). Recently, two p53-bound enhancers were shown to produce eRNAs locally that regulate a more distal coding gene (Melo et al., 2013). However, it remains unclear whether transcription in the vicinity of p53 REs is common and whether such events are regulated.

Here, we use chromatin immunoprecipitation followed by exonuclease treatment (ChIP-exo) (Rhee and Pugh, 2011) to precisely and more accurately map the genomic locations of p53 binding in response to a variety of genotoxic stresses. ChIP-exo is a refinement of ChIP-seq that produces high accuracy and sensitivity. From this, we characterize the surrounding DNA sequence and target genes. To investigate potential transcription events in the vicinity of p53, we mapped transcription factor IIB (TFIIB) and polymerase (Pol) II by ChIP-exo, measured RNA, and examined their function at select model genes, all in response to a variety of stresses (UV light, nutlin, doxorubicin, and 5-fluorouracil). Together, these findings uncover a pervasive and comprehensive network of coding and noncoding transcription that is stress induced and p53 regulated. Collectively, these results implicate p53 in playing a broader role in "guarding" the genome.

RESULTS

Detection of 2,183 p53-Bound REs

We first examined p53 binding in U2OS cells 6 hr after UV treatment, which we confirmed to induce signatures of apoptosis and responses to DNA damage (Figure S1A). Later in the study, we also employed other p53-activating agents (Figure S1B). The distribution of p53 ChIP-exo tags (5′ ends) under conditions of UV stress for all candidate locations is shown in Figure 1A. To achieve comprehensive coverage while maximizing accuracy (Table S1), we implemented a bioinformatic validation/filtration approach to ferret out false positives (Figure S1C). Remarkably, ~90% of all locations were validated as having a 20 bp unsplit RE, which included 4% having a 1 bp spacer. The false discovery rate was <5%, determined by scrambling the motif or the search space. A triple peak pair pattern was evident around the REs (Figure 1B). Each peak pair corresponded to a p53/RE half-site border (Figure 1B, upper diagram), with the central peak pair reflecting the adjoining internal borders between adjacent half-sites. This pattern reflects on a genomic scale the crystallographic structure of p53 as a dimer of dimers (Kitayner et al., 2006; Tidow et al., 2007) and offers a potential diagnostic signature for p53 binding across a genome.

When all examined stresses were considered, 2,183 p53-bound REs were found. More may remain undetected in other cell types or responses. Consistent with prior reports of inducibility of p53 binding (Ceribelli et al., 2006; Espinosa et al., 2003; Kaeser and Iggo, 2002; Shaked et al., 2008), about half of all p53 locations had a >2-fold change in occupancy in at least three of the four stresses (Figure 1C; Table S1, which allows occupancy thresholds to be adjusted). Thus, about half of p53-bound REs appear to be activated via a general stress response, which is consistent with the concept of a core default response (Nikulenkov et al., 2012). About 30% were specific to two stresses, and 15% were specific to either 5-fluorouracil or UV treatment. Both nutlin and doxorubicin elicited a general response but little or no detectable stress-type-specific response. This was also apparent at higher fold change thresholds (Figure S1D) and, thus, differs from a prior conclusion that there may only be a single default response (which was defined in a different cell line) (Nikulenkov et al., 2012). Moreover, nutlin and doxorubicin were not entirely identical, which is in accord with a prior report by Menendez et al. (2013).

As expected, the set of ChIP-exo locations determined under UV stress substantially overlapped with nine preexisting data sets of locations determined by ChIP-chip, ChIP paired-end tags, and ChIP-seq (Figures S1E and S1F). However, about 36%–95% of prior locations were not found in our UV-induced data set, and similar percentages were missed. The number of locations identified here and in other studies is subject to differences in cell types, stress treatments, levels of nonspecific DNA contamination, assay variables such as PCR amplification, and data thresholding, all of which places substantial limits on the generalization of conclusions drawn.

RE Sequences Are Degenerate, Unsplit, and Spatially Organized in the Genome

Only 162 (10%) of all p53-bound REs detected in U2OS cells contained an exact match to an already degenerate 20 bp full RE consensus (RRRCWWGYYYRRRCWWGYYY), thereby precluding effective ab initio site identification without having measured binding locations. p53-bound REs typically contained one half-site that matched the consensus (Figure 1A) and a second half-site that deviated from the consensus by a limited degree. This observation fits with prior studies by el-Deiry et al. (1992) and Funk et al. (1992) and with the notion that p53 initiates binding at one half-site then completes binding at a second half-site (McLure and Lee, 1998). p53 was not appreciably detected at isolated half-sites and, thus, may only stably bind full sites in vivo.

Binding was the lowest, but also the most inducible, at weak REs (Figures 2A and S2A). Deviations from the consensus quarter site ($R_1R_2R_3CW$) followed the trend: $R_1 > R_2 > R_3 = W > C$, with the central two quarter sites being somewhat less variable for their respective half-sites (Figures 2B and S2B). Therefore, basal and constitutive p53 site occupancy may be tuned in part through variations from the consensus.

Although p53 is thought to bind REs that contain 1–13 bp insertions between their half-sites (el-Deiry et al., 1992; Funk

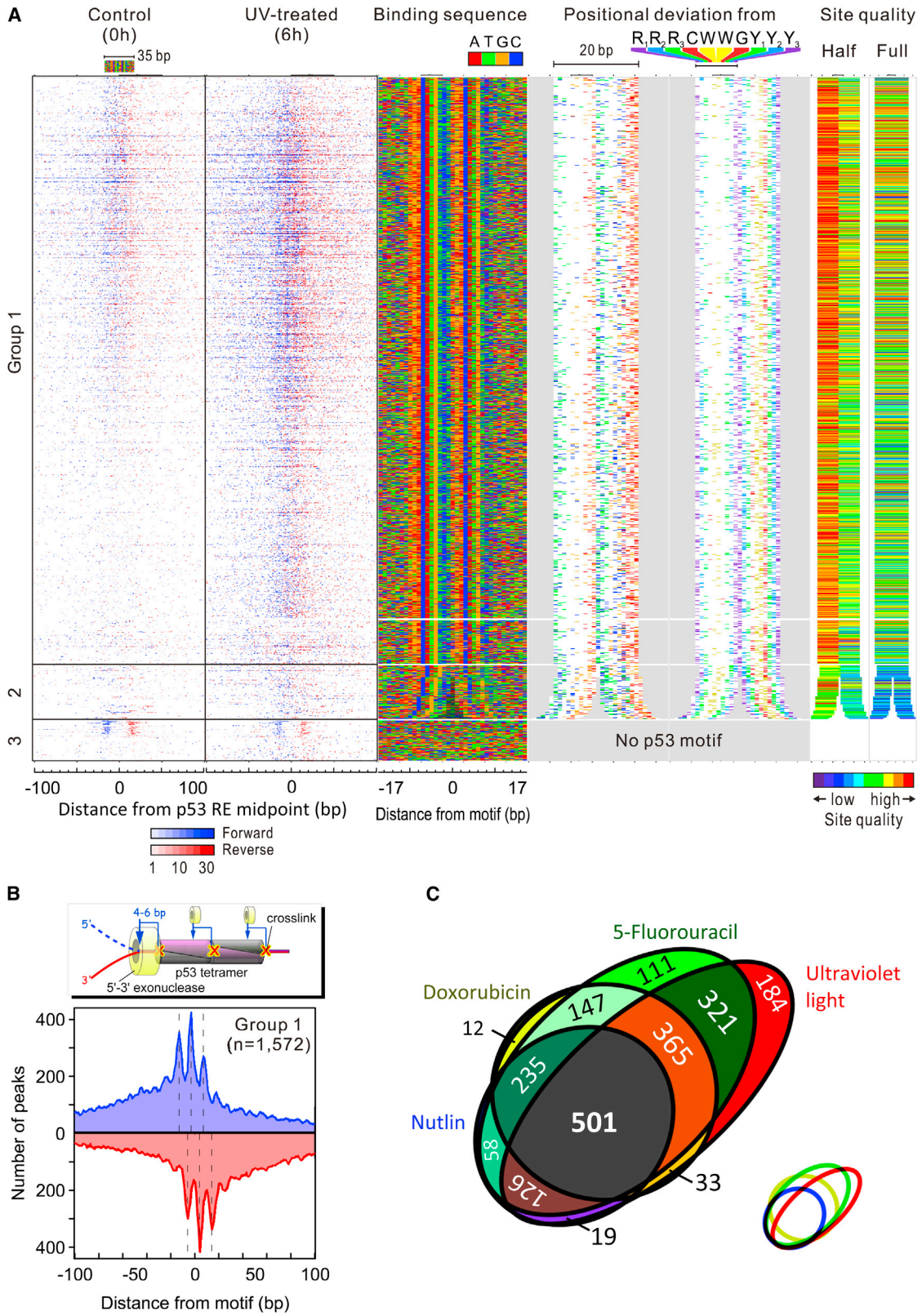

(legend on next page)

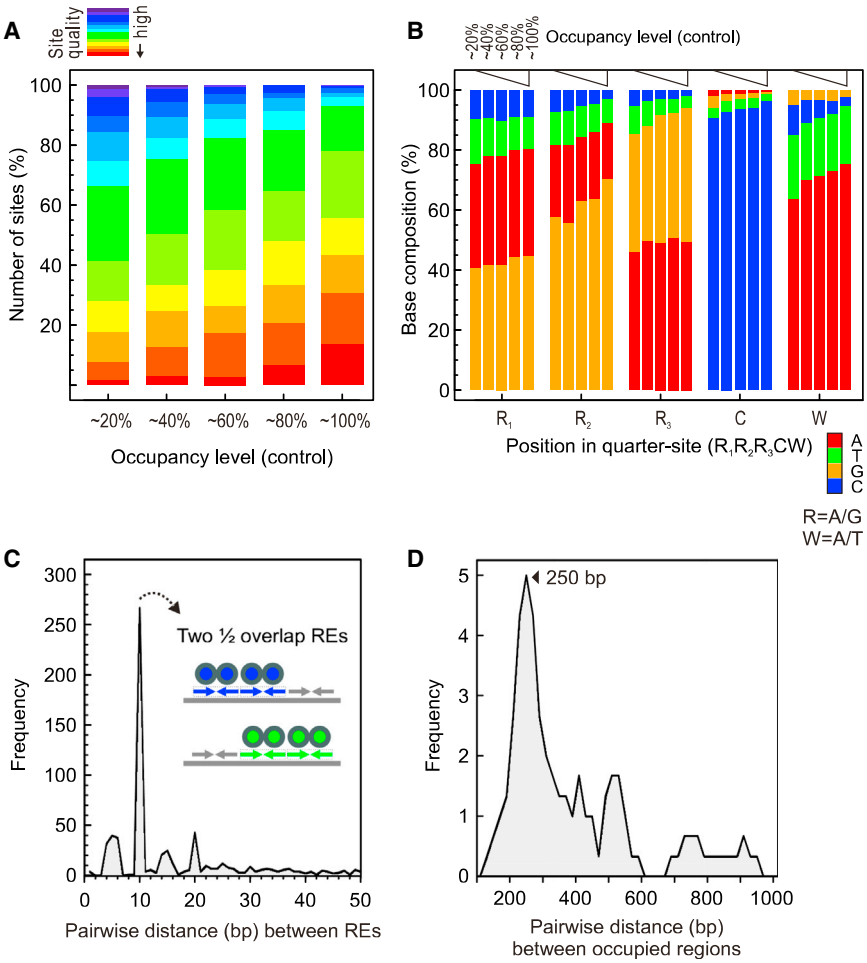

Figure 2. Genome-wide Characteristics of p53/RE Interactions

(A) Relationship between p53 site quality and occupancy level. U2OS group 1P sites (n = 1,452) were binned according to occupancy levels (percentages) in uninduced cells, then color coded according to site quality (according to Menendez et al., 2009). Blue is further from the consensus.

(B) Base composition at each position in an RE quarter site (RRRCW), separated out by occupancy levels (percent ranks) in uninduced control U2OS cells.

(C) Frequency distribution of pairwise distance between p53-bound REs. A total of 2,129 REs in 1,571 group 1 regions were subjected to autocorrelation analysis.

(D) Frequency distribution of pairwise distance between p53-occupied regions. A total of 1,571 group 1 regions were subjected to autocorrelation analysis. Multiple REs in a region were treated as a single location. Data were binned in 20 bp intervals and smoothed using a three-bin moving average. A total of 40 paired regions were <600 bp apart.

et al., 1992; Jordan et al., 2008; Qian et al., 2002; Riley et al., 2008), these events were rare (n = 67; Table S1) and could be explained by weak unsplit sites that overlap with seemingly stronger but erroneous split sites (Figures S2C and S2D). We therefore conclude that p53 tetramers bind only to unsplit REs.

A large number of closely spaced REs overlapped by 10 bp (n = 267 pairs; Figure 2C). This affords p53 with two binding sites at the cost of evolving three half-sites. Overlapping sites had the same distribution of sequence quality as nonoverlapping sites (data not shown) but tended to be constitutively occupied (Figure S2E). A second mode of RE site clustering was observed with an ~250 bp separation (Figure 2D). Thus, p53-bound REs have both a local and a distal positional relationship with themselves.

Binding Sites for p53 and Other Cellular Factors Have Positional Relationships

Because p53 interacts with sequence-specific transcription regulators and the core transcription machinery (Laptenko and Prives, 2006), we expected to detect p53 crosslinking to other proteins bound at their cognate DNA sites. But this was not observed. We therefore searched for DNA motifs that co-occurred with REs as one indicator of factors that might work positively or negatively with p53 locally. Several motifs were not only enriched near p53 REs, but many peaked at fixed distances and had a fixed orientation relative to the REs (Figures 3 and S3A). For example, p53-bound REs displayed a peak of enrichment 30 bp 3′ to the GATA1 motif, WGATAR, thereby implicating at least one GATA family member in coregulation with p53. Other positional relationships included factors involved in environmental stress and oncogenesis, such as

Figure 1. Comprehensive Identification of p53-Bound REs in UV-Treated U2OS Cells

(A) Distribution of 5′ ends of p53 ChIP-exo sequencing tags around all 1,824 enriched regions (rows) detected in untreated or UV-treated U2OS cells. Data are in three groups, having (1) two RE half-sites with no insertion (n = 1,571), (2) two putative RE half-sites with 1–13 bp insertion or 1 bp deletion (n = 146), or (3) all others (n = 107). REs are oriented to have the stronger consensus half-site to the left. Data are normalized to a global constant background. Rows are linked across all panels and sorted by fold change in p53 occupancy. The third panel displays the DNA sequences encompassing each RE. Group 3 used the peak pair midpoint. The fourth panel reports only deviations from the consensus, using the same color code as in panel 3. The fifth panel reports the same deviations using position-specific colors. The far-right panels report half- or full site quality, as a whole, based on transactivation potential (Menendez et al., 2009).

(B) Composite distribution of the locations of p53 ChIP-exo peaks for Group 1, distributed around RE midpoints and smoothed with a 3 bp moving average. The model shows an interpretation of the ChIP-exo peak pattern. In a population of p53/RE tetramer complexes, crosslinks occur at the tetramer edge and internally between dimers. Because crosslinking is incomplete, a more 5′ crosslink (denoted by "X") does not necessarily block detection of a more 3′ crosslink in a population-based analysis.

(C) Venn diagram of p53 binding locations responding to stress (at least 2-fold occupancy change).

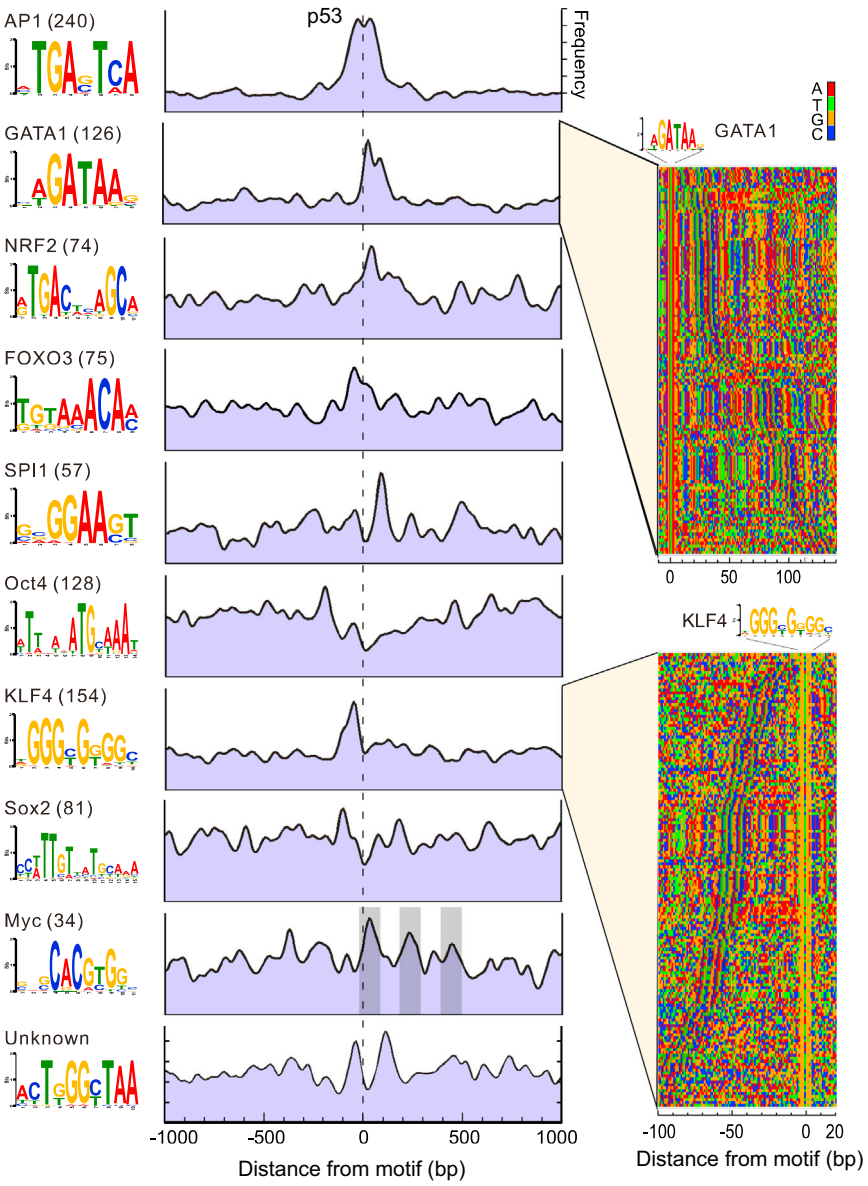

Figure 3. Stress-Response Elements Have a Spatial Relationship with REs

MEME logos of motifs statistically enriched near the 1,571 p53-bound regions of group 1, along with the number of occurrences. The distribution of p53/REs around each motif (motif $p < 10^{-4}$), orientated according to the sequence logo, is shown. The composite plot uses a Gaussian kernel and a smoothing bandwidth of 20. Four-color nucleotide plots for each instance of the indicated motifs (GATA1 and Klf4) are shown to the right, in which p53 REs are shaded.

AP1, NRF2, FOXO3, and ETS/SPI1/PU.1, and pluripotent stem cell maintenance, such as Oct4, Sox2, Klf4, and Myc, or related family members. A number of these factors have been demonstrated to have functional interrelationships with p53 (Renault et al., 2011; Rotblat et al., 2012; Tu et al., 2009; Zhu et al., 2006). Approximately 1,000 paired genomic features were identified (Table S2).

A substantial subset of these features exists within ancient endogenous retroviral long terminal repeats (LTRs) (see blocks of vertical colored stripes in the right panels of Figure 3, and also Figure S3B), which may contribute to positional specificity. Because AP1 and NRF2 were positionally restricted, but not enriched in repetitive elements, positional constraints of some elements were not necessarily a consequence of being in repetitive elements. Moreover, element had the same orientation relative to REs regardless of whether it was inside or outside of LTRs, indicating that such constraints are not imposed by the LTR. LTRs are among the oldest repetitive elements in the human genome, and thus, the maintenance of factor binding sites is likely to be important. These findings are entirely consistent with and expand upon the concept that endogenous LTRs act as enhancer vehicles (Cohen et al., 2009). Together, the distance and orientation constraints of the motifs suggest that a spatial, potentially cooperative, relationship exists between many p53/RE complexes and the factors (or complex of factors) that bind to the identified motifs. A cooperative relationship would reduce the dependence of p53 on the RE sequence.

TFIIB and Pol II Are Enriched at REs

With the discovery of eRNAs and, in particular, a recent report of two p53-bound RE regions giving rise to eRNAs (Melo et al., 2013), we next addressed the generality of RE-associated transcription in the context of all 2,183 p53-bound REs. We performed ChIP-exo on the general transcription initiation factor TFIIB and RNA Pol II, as well as strand-specific RNA sequencing (RNA-seq). Remarkably, TFIIB tags were enriched at p53 REs across multiple cell lines (Figure S4). When all data were merged, the enrichment was evident at most p53 REs (Figure 4A). Similar enrichments were observed for Pol II and, to a lesser extent, RNA (Figure 4A). The occupancy levels of both TFIIB and Pol II at most locations were similar to the average at annotated mRNA genes (tag counts: TFIIB, 4.3/2.6/2.1; Pol II, 6.3/7.0/2.1, for RE-associated/mRNA/"+100 kb" background, respectively, as defined in Figures 4B and 4C).

A composite plot of TFIIB occupancy at all REs, orientated to place the higher level of TFIIB on the same side, shows that TFIIB was particularly enriched within 50 bp of an RE midpoint (Figure 4B). This was confirmed by the Pol II data, which was orientated based on TFIIB (Figure 4C). We interpret this enrichment as

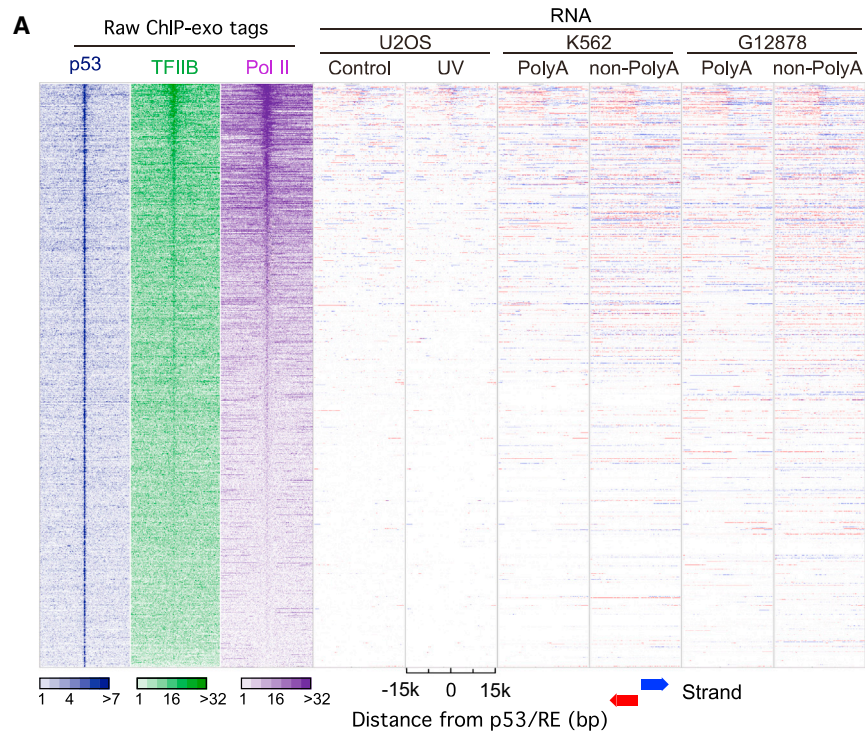

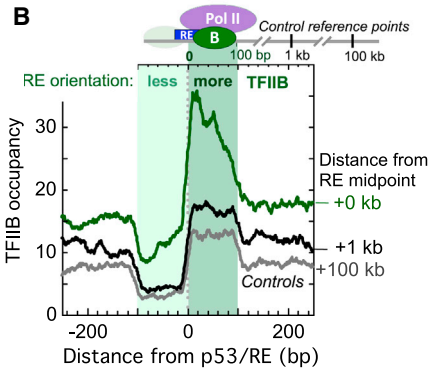

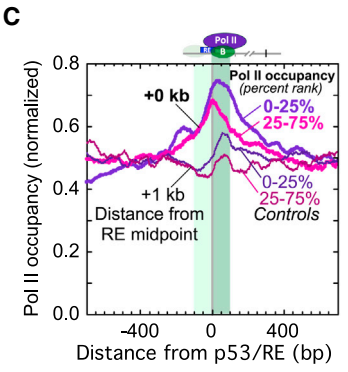

Figure 4. p53/REs Coincide with Noncoding Transcription Complexes

(A) Plot of p53, TFIIB, and Pol II ChIP-exo tag 5′ ends around individual REs (rows). All data from U2OS and HCT116 cells were combined. All rows are linked, aligned by RE midpoint, plotted from ±15 kb, and sorted by Pol II occupancy (in the ±2.5 kb region). ChIP-exo data were normalized to have a constant total background (not locally normalized). Also shown are corresponding RNA-seq tags, parsed by DNA strand (blue denotes 5′–3′ from left to right; red denotes the antiparallel strand). RNA-seq data from K562 and G12878 cells were added for comparison (Morozova et al., 2009). Please note that the orientation of each pair of DNA strands is random, which gives the false impression of transcription bidirectionality.

(B) Composite distribution of TFIIB around 2,183 p53/REs or control regions (+1 and +100 kb from each RE). REs were orientated to maximize TFIIB occupancy on the right. All data sets (cell lines and stresses) for each factor were combined.

(C) Composite distribution of Pol II, orientated as in (B), and broken out into occupancy percent ranks. This subdivision necessitated normalizing the data.

sites of local initiation complex assembly that are positionally linked to p53 REs. Because <1% of p53 REs are within ~100 bp of an annotated mRNA transcription start sites (TSSs), the local p53-associated initiation complexes may produce noncoding transcription. However, whereas soluble/stable RNA levels appear to correlate with Pol II levels over the broader region (Figure 4A), TSS detection appeared limited to high-occupancy initiation complexes. Therefore, it remains unclear whether low-occupancy sites are indeed sites of initiation, as opposed to sites of initiation complex assembly.

Stress-Induced RE-Associated Transcription Complexes

We next examined whether RE-associated transcription complex assembly was regulated by the same environmental stresses that regulate the p53 response. Relative to unstressed control cells and compared to an equivalent set of randomly selected annotated genes, treatment with nutlin-3a, doxorubicin, or 5-fluorouracil resulted in a substantial number of p53 RE regions showing a >4-fold increase in TFIIB and Pol II occupancy (Figure 5A). However, this was more evident in HCT116 $p53^{-/-}$ cells. In HCT116 $p53^{+/+}$ cells, more RE regions saw a decrease in TFIIB/Pol II occupancy in response to stress. In U2OS cells, which have an intermediate level of p53 (Figure S5A), an intermediate effect was observed. Although conclusions that can be drawn across distinct cell types may be limited, the results suggest that a variety of stresses induce local RE-associated transcription complex assembly, but the levels of these complexes are generally reduced at high levels of p53. Very different mechanisms could explain the reduction. First, due to its proximity, p53/RE binding might directly block assembly, although an indirect mechanism is not excluded. Alternatively, p53/RE binding might release the initiation complex into productive transcription thereby dissipating Pol II from the region, and a loss of TFIIB. Other mechanisms are not excluded. How transcription complex assembly arises in the absence of p53 is unclear, although one suggestion from Figure 4 is that other nearby transcription factor binding sites and their cognate factors could fulfill this role.

The observation that nutlin treatment, like other stresses, resulted in a substantial number of TFIIB and Pol II RE-associated locations increasing in occupancy in the absence of p53 (HCT116 $p53^{-/-}$) was surprising because nutlin is thought to block Mdm2-p53 interactions, which are absent

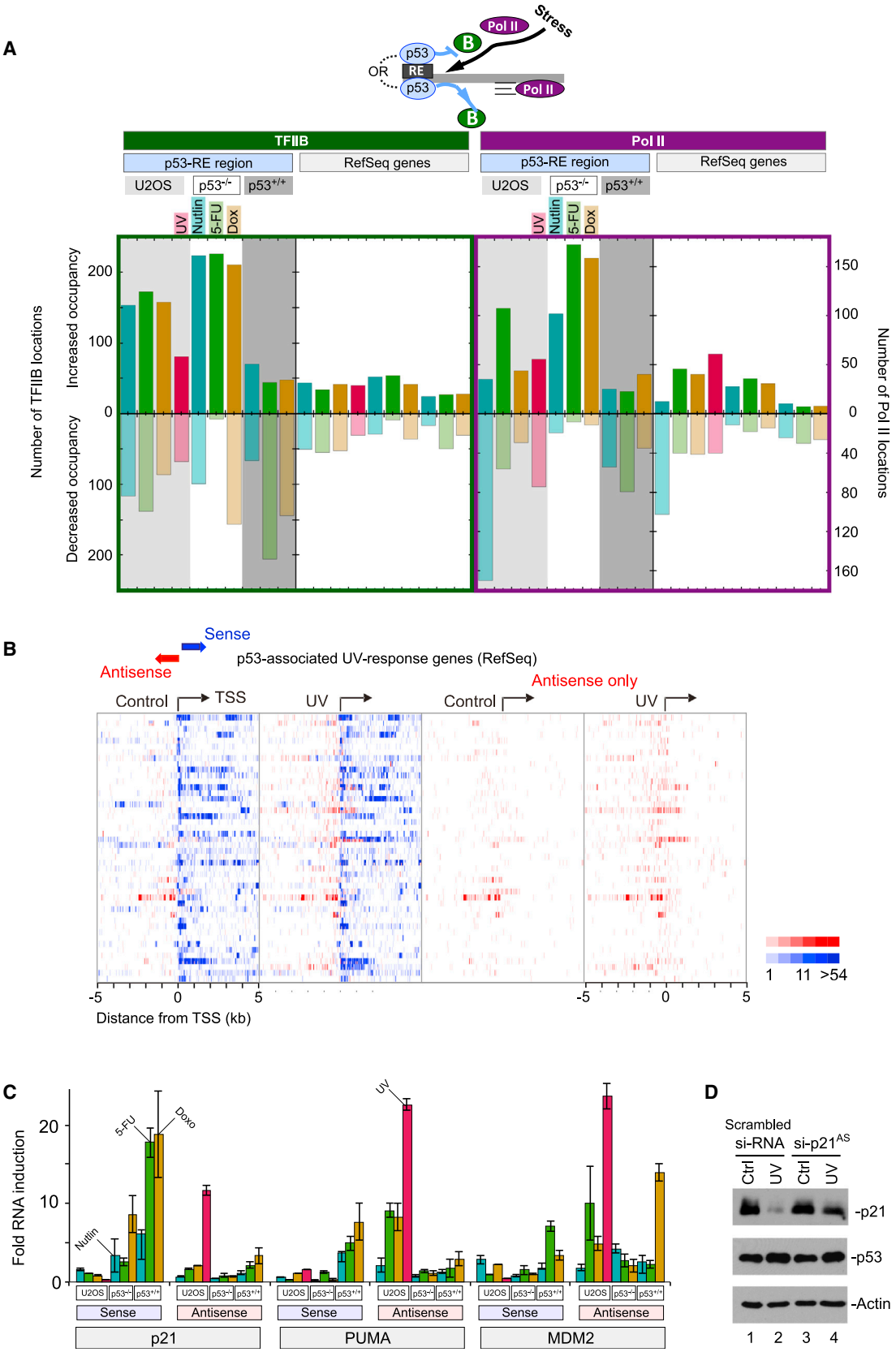

(legend on next page)

in this cell line. Recent studies suggest that other Mdm2 interactions are also inhibited by nutlin, independent of p53 (Kurokawa et al., 2013; Valentine et al., 2011). If true, disruption of such interactions by nutlin might promote assembly of TFIIB/Pol II at REs.

Surprisingly, in U2OS cells, 46 RE-associated UV-induced annotated genes (described below) produced antisense transcripts (Figure 5B; Table S3), many of which were also UV induced. These included the well-studied *p21*, *PUMA*, and *MDM2* genes (Figure S5B), which we verified by quantitative PCR (qPCR) (Figure 5C, red bars). Other stresses also caused antisense induction at these three genes. Antisense RNA levels were generally greater than sense RNA levels. In HCT116 cells having high levels of p53, the relative sense/antisense inducibility was largely reversed, where sense transcription was more highly induced. Cells lacking p53 did not display a biased sense/antisense relationship (except at p21). These findings suggest that at least at *PUMA* and *MDM2*, high levels of p53 may inhibit stress-induced antisense transcription and promote sense transcription, thereby regulating sense/antisense ratios. A similar mechanism may be in play at *p21* but with additional p53-independent contributions. Thus, p53 levels may affect the expression of coding genes in part through effects on antisense transcription. This assessment is based on general trends of p53 levels occurring across distinct cancer cell lines and within the same cell line and, thus, complicated by cell-type-specific effects.

To directly address the role of antisense in regulating sense expression, *p21* antisense transcripts were knocked down in U2OS cells by small interfering RNA (siRNA), then tested for *p21* sense induction by UV stress. We observed an increase in levels of *p21* protein in comparison to a scrambled siRNA control (Figure 5D). This suggests that UV-induced *p21* antisense RNA downregulates *p21* sense expression, in accord with a prior report demonstrating that UV stress leads to reduction of *p21* in preparation for apoptosis (Bendjennat et al., 2003). It also fits with the more general notion that p53-regulated noncoding RNA (ncRNA) promotes gene repression globally (Huarte et al., 2010; Marín-Béjar et al., 2013). Taken together, these findings suggest a tandem repression mechanism for regulating *p21* expression, where stress-induced antisense transcripts attenuate stress-induced sense expression. High levels of p53 may inhibit antisense production, thereby allowing full sense gene activation (which may also have direct contributions from p53 and other factors). How general this mechanism is remains to be determined because not all stress-induced antisense transcription is accompanied by a corresponding reduction of sense transcription (Figure 5B).

p53-Associated Stress-Induced Genes

In an effort to link p53 and stress with mechanisms of gene regulation, we initially narrowed in on a filtered set of 751 "active" genes (annotated TSSs having stringently defined TFIIB, and also being <10 Mb from a p53-bound RE in UV-treated U2OS cells; see Supplemental Experimental Procedures for details and Table S4). UV treatment of U2OS cells generally had little effect on TFIIB occupancy at these genes, which was surprising because recruitment of initiation factors has been considered as one basis for gene induction (Ma, 2011; Ptashne and Gann, 1997). In contrast, Pol II was released from where it normally pauses at the 5′ ends of genes and increased in gene bodies, which is in accord with models on heat shock induction (Figure S6A) (Rougvie and Lis, 1988). We cannot exclude the possibility that at least some of the Pol II is lost due to UV-induced degradation. Related observations of Pol II release were reported at the p53-regulated Fas and p21 genes (Espinosa et al., 2003; Gomes et al., 2006), but this has not been examined on a genomic scale.

The reduction of Pol II at promoter regions generally diminished at longer p53 distances from the annotated TSS (Figure 6A), indicating that proximity to p53 is associated with UV-induced Pol II release from the pause region. Consistent with the role that distance plays, only the two closest "active" genes to p53 REs tended to respond positively to UV stress, in comparison to more distal genes that responded negatively (Figure 6B). Although these findings do not establish that p53 directly participates in the pause release, and there are certainly p53-independent UV-mediated effects on Pol II, they are consistent with established interactions of p53 with elongation factors (Lew et al., 2012; Shinobu et al., 1999), which include c-Myc (Rahl et al., 2010). As noted in Figure 3, binding sites for the pausing regulator c-Myc are organized around p53 REs.

Using the proximity assessment described above, we generated a set of 269 "active" annotated genes having p53 binding within 15 kb of their TSSs but also having a lower stringency for TFIIB occupancy (see Supplemental Experimental Procedures), so as to be more inclusive of potential p53-regulated genes. Of these, p53 was particularly enriched within 1 kb of the TSS of 48 mRNA, 14 ncRNA, and 6 tRNA genes (Figure 6C). These promoter-proximal p53 locations generally had REs that deviated more from the consensus than distant REs (Figure 6D), which is a property of more inducible REs.

Within this set of 269 genes, we identified 151 mRNA genes in which UV treatment was linked to increases in Pol II in the body of the gene (Figure 6E; Table S5). As demonstrated above, this might reflect some net contribution of sense and antisense transcription. Table S5 also reports hand-selected literature-curated alternative targets, which did not meet our objective criteria for

Figure 5. Impact of Stress and p53 on TFIIB and Pol II Occupancy and RNA Levels

(A) Number of p53/RE locations (out of 2,183) that increases or decreases in TFIIB or Pol II occupancy by more than 4-fold upon the indicated stress treatment in U2OS and HCT116 ($p53^{-/-}$ and $p53^{+/+}$) cells. Also shown is a parallel analysis with randomly selected RefSeq promoter regions (typically not p53 regulated), representing the false-positive rate. Occupancy levels were first normalized to globally averaged local background.

(B) Distribution of sense (blue) and antisense (red) RNA within 5 kb of a p53-associated mRNA TSS (n = 40) that displays a sense/antisense relationship. The first two panels overlay sense and antisense in control and UV-treated U2OS cells, whereas the third and fourth panels show only the antisense.

(C) qPCR detection of sense and antisense transcripts at three p53-regulated genes in response to stress (n = 3). Values represent fold changes in RNA relative to unstressed controls. SDs are shown.

(D) Knockdown of p21 antisense transcript results in elevated p21 levels. U2OS cells were treated with either p21 antisense siRNA or with a scrambled siRNA, then subjected to mock or UV treatment. Western blotting of p21, p53, and an actin control was then performed.

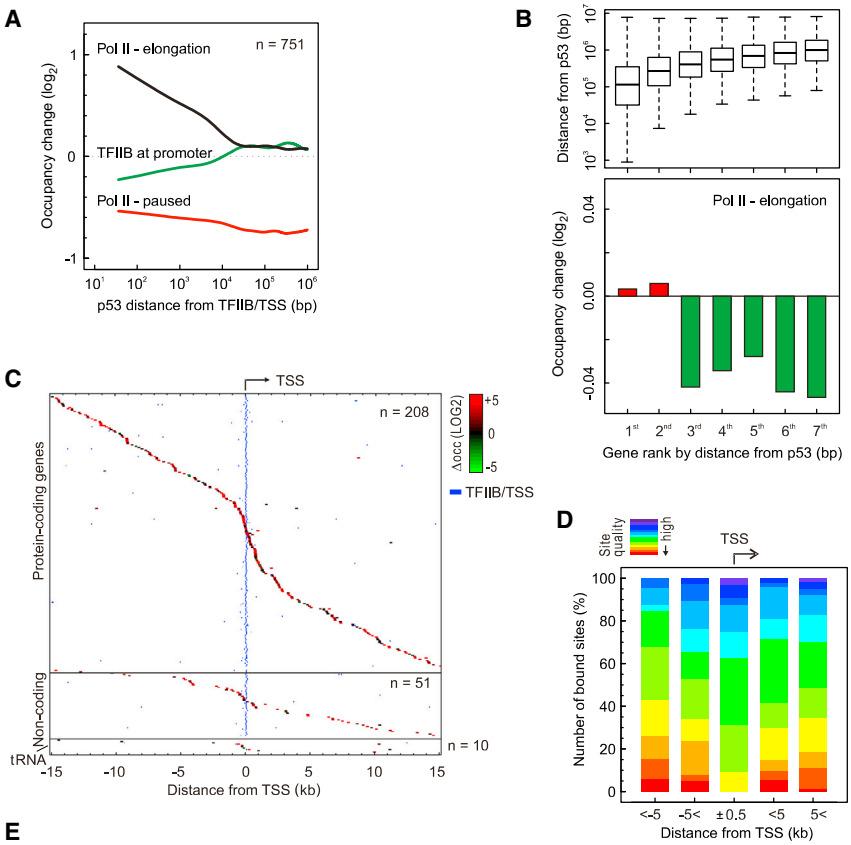

Figure 6. Properties of p53 at Annotated Genes

(A) Fold changes in TFIIB or Pol II occupancy, upon UV treatment in U2OS cells, are shown as a function of distance between TFIIB/TSS locations and the closest p53.

(B) Bar graph of changes in median Pol II occupancy in 751 "active" gene bodies in response to UV treatment in U2OS cells as a function of ranked order distance from p53 (bottom graph). Distances of their TFIIB/TSS locations from the nearest p53 are indicated in the top panel.

(C) Distribution of p53-bound locations within 15 kb of 269 annotated TSS/TFIIB locations (blue). Rows were sorted by p53-TSS distance. Each p53 location was color coded according to its changes in occupancy in response to UV treatment.

(D) Site quality of p53 REs in relation to distance from TSSs. p53-bound REs within the indicated range of a HAVANA TSS/TFIIB location (n = 252) were obtained, then the fraction of sites was color coded according to site quality, as in Figure 2A.

(E) List of "active" p53-associated genes that showed increased Pol II binding in their gene body (from Table S5). Underlined genes are known to be p53 regulated.

E

Categories of UV stress-induced genes linked to p53-bound locations

Apoptosis Cell cycle		DNA Repair Chromatin	Cell growth Differentiation	Transcription Regulation	Signal Transduction		Cell Adhesion Mobility	Biosynthesis Metabolism		Transportation Membrane Homeostasis	Unknown
BRMS1	PCNA	ASCC3	ACYP2	ATF3	AKAP10	S100A16	ACTA2	CAPN2	MRPL36	ABCD3	C11orf24
BAX	PGF	DDB2	DYRK3	CSDA	ARVCF	SDC4	ASTN2	CES2	NT5M	ACBD5	C20orf30
BTG2	PHLDA3	DGUOK	FBXO15	DDIT3	C10orf10	SERPINE1	MTBP	COX6A1	OPLAH	ARC	C20orf72
BTG3	PLK3	GPX1	FBXO22	FHL2	DUSP11	TBC1D22B	PLK2	DCP1B	PANK2	BLOC1S2	CCDC51
CCDC72	PTP4A1	KDM5C	GLI4	FOSL1	DUSP7	TBK1	PVT1	DGAT1	RPLP2	C18orf55	CCDC58
CCNG1	S100A6	LMNA	IER5	MED21	FGFR2	TM7SF3	RAP2B	EXOSC4	SARS	C3orf52	FAM200A
CDKN1A	TIGAR	METTL8	KRT17	RARA	HRH1	TMEM183A		GATC	SDF4	FTL	KIAA0247
EPHA2	TRAF4	POLH	MRPL13	SERTAD1	IPO9	TMEM68		GPAA1	UBR5	GCC2	RBM12B
GADD45A	TRIAP1	RAD51C	MRPL14	TGS1	JAG1	TRIM5		GTPBP5	UTP3	SDAD1	TP53TG1
OGT		RRM2B	PUM2	ZNF219	KLRG1	VGF		LASS5	WDR43	SEC31A	Novel (2)
		SETD1A	SESN2	ZNF337	LRRC28			LRP1	ZC3H7B	SLC12A4	lincRNA (3)
		TET2		ZNF488	RBM14			MDM2		SNAP47	ncRNA (16)
		XPC		ZNF655						TSNARE1	
										VPS24	

gene activity. An additional lower-confidence set of 100 genes, having UV-induced p53 binding >15 kb away and displaying increased Pol II binding in the gene body, is provided in Table S6. These were not studied further. In Table S1, we also report the closest annotated gene (including annotated ncRNAs) to each of the 2,183 p53/REs regardless of their transcriptional activity. Many of these may be bona fide p53 targets but did not meet our measured criteria of gene activity.

The 151 high-confidence genes in Table S5 include 74 previously reported p53 target genes, whereas 77 genes were not previously identified as being linked to p53, which demonstrates the utility of this study in identifying new transcription factor target genes. Several new target genes include long intergenic RNAs (lincRNAs) and transcripts of unknown function (Figure S6B). Several lincRNAs have been previously identified as p53 targets (Barsotti and Prives, 2010; Huarte et al., 2010). They play a key role in p53-mediated repression of genes on a broad scale. The newly assigned p53 target genes are involved in a variety of functions, including cell growth, cell cycle, cell signaling, differentiation, apoptosis, cell adhesion and motility, and intracellular transportation (Figure 6E; Table S5).

p53/RE-Associated Genes Dominate Stress Regulatory Networks

Gene network analyses found that the DNA replication, recombination, and repair gene network had the highest enrichment score ($p \approx 10^{-48}$) (Figure 7A). Of the 25 genes involved in this network, 10 of them are newly discovered p53 targets. The functions of these genes implicate p53 in regulating many more steps of the DNA-damage response after UV irradiation than previously appreciated. Of the existing and novel targets, CDKN1A, GADD45, and PLK3 control the cell cycle, allowing time to repair damaged DNA before the cell cycle progresses further. XPC and DDB2 recognize damaged DNA and recruit the DNA-damage repair complex. POLH, PCNA, and UBR5 repair the damaged DNA. FTL and RRM2B can participate in the synthesis of deoxyribonucleotides for DNA repair. Several factors regulating p53 posttranslational modifications (e.g., PLK3, MDM2, MTBP, and OGT) are present in this network, suggesting that p53 feedback loops are activated to repair DNA damage. RAD51C in the DNA-repair network is related to RAD51, an important mediator of homologous DNA recombination

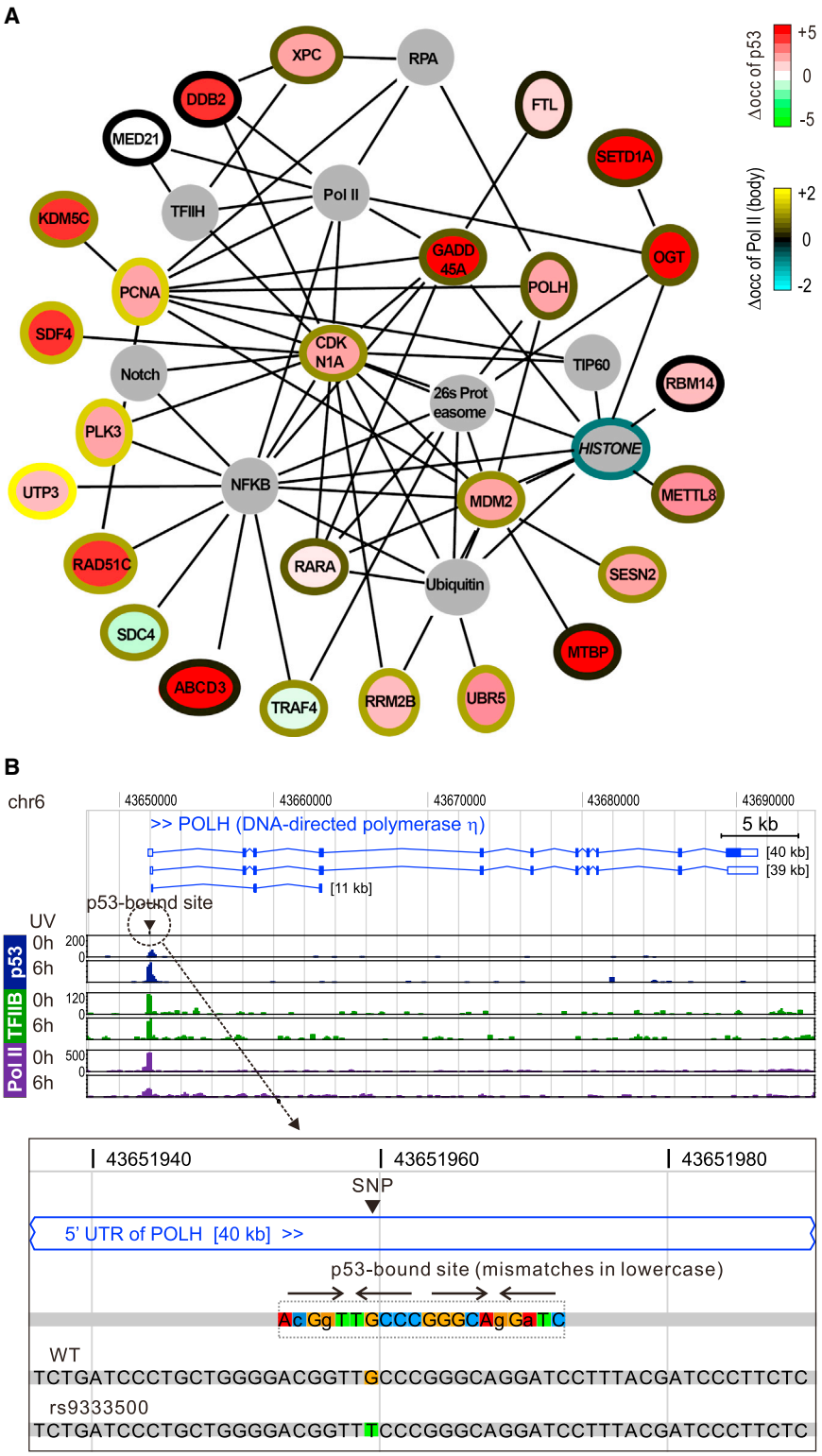

Figure 7. p53 Regulatory Networks and SNPs

(A) Known IPA (Ingenuity Pathway Analysis) DNA-repair network of gene/protein (nodes) interactions (edges). Nodes are colored shades red or green to reflect fold changes (increased and decreased, respectively) in p53 occupancy upon UV treatment. Relative change in Pol II occupancy in the gene body is marked by yellow/cyan-shaded (up/down) halos encompassing the nodes. Gray indicates that a p53/RE was not assigned to these genes.

(B) Browser shot of the POLH gene, displaying UV-induced p53 binding at an RE that contains a SNP as a common variant. The lower panel displays a blowup of the bound p53 RE, identifying the location of the rs9333500 SNP at the seventh G position.

repair. RAD51 is reportedly p53 repressed (Arias-Lopez et al., 2006), whereas we show here that RAD51C is induced, which suggests differential usage of these recombinases during a UV stress response. As such, this network regulates p53 itself, the cell cycle, nucleotide excision repair, and homologous DNA recombination repair.

Another highly scored network regulates cell death and survival, with 12 out of the 22 genes in this network being new p53 targets (Figure S7). Genes for growth factors and their receptors, such as *FGFR2*, *VGF*, *PGF*, and *JAG1*, were identified. Notably, p53 may also directly regulate *FOSL1*, encoding an AP1 family transcription factor that was recently discovered as a target of JQ1 in lung cancer cells (Lockwood et al., 2012). As shown in Figure 3, AP1 sites are also positioned next to p53 sites. This represents a link of p53 with cell growth and survival regulation. Genes with growth inhibition functions were also identified, such as *DUSP7*, *BTG2*, and *BTG3*. In general, genes within this network regulate cell growth, cell death, and survival, consistent with p53 being important in maintaining tissue homeostasis after DNA-damage recovery. The role of p53 in metabolism has been more recently studied by Vousden and Prives (2009). Within the metabolism network, 12 out of the 17 genes were newly identified p53 targets (Figure S7). These include genes regulating RNA stability and degradation (e.g., *EXOSC4*, *DUSP11*, and *PUM2*), protein degradation (e.g., *FBOX15* and *FBOX22*), and mitochondrial functions (e.g., *COX6A1*, *MRPL36*, and *PANK2*). Notably, PANK2 is a master regulator of coenzyme A synthesis in mitochondria, the genetic alteration of which is linked with neurodegenerative diseases (Zhou et al., 2001).

With a comprehensive and accurate map of p53-bound REs, we sifted through the National Center for Biotechnology Information (NCBI) dbSNP database (build 130 having 13,864,001 SNPs) (Sherry et al., 2001) in search for any SNPs that overlapped with a p53 RE. We found one SNP (rs9333500) that was of particular interest because it resided in a UV-inducible p53-bound RE that we associated with the polH gene (Figure 7B). UV treatment resulted in increased Pol II occupancy in the gene body of *POLH*. This gene encodes the DNA-directed DNA Pol η and has been reported to be upregulated by DNA damage in a p53-dependent manner (Liu and Chen, 2006). polH conducts translesion DNA synthesis through UV-induced pyrimidine dimers. Defects in this gene result in xeroderma pigmentosum, displaying hypermutability after exposure to UV irradiation and resulting in skin malignancy (Loeb and Monnat, 2008; Masutani et al., 1999). The rs9333500 SNP results in a change from G:C to T:A at position 7. This is the "C" position in the RRRCW quarter site that is internal to the RE, which is the least variable position within the least variable quarter site. Surprisingly, the other quarter site within the same half-site contained a nonconsensus "G" at position 4 (in RRRCW). Thus, this RE is expected to be intrinsically weak and inducible. The rs9333500 SNP is expected to eliminate p53 binding, altogether. rs9333500, which is homozygous in ~2% of the human population (PDR90), is expected to render these individuals sensitive to UV-induced DNA damage.

DISCUSSION

p53 Has a Single Predominant Mode of Binding across the Human Genome

Our results point to the existence of about 2,200 p53/RE complexes spread across the human genome, most of which increase in occupancy in response to stress. ChIP-exo detects p53/RE interactions as a triple peak pair pattern that may serve as a useful diagnostic for p53 binding. We found no convincing evidence for p53 binding to DNA sequences other than to a 20 bp unsplit RE that can have some degree of degeneracy, based on the following reasoning and evidence. Putatively split REs, having 2–13 bp spacers between two half-sites, may actually be degenerate unsplit sites that have one half-site below the threshold of detection. Candidate p53 locations that we deemed to be incorrect were infrequent and had low p53 occupancy and, thus, were near the limits of detection. They lacked definitive properties that include well-defined peaks and a well-defined motif centered between peak pairs. Enriched motifs in their vicinity were CT rich, making them similar to motifs enriched in so-called "blacklisted" regions of the genome. Such regions tend to give artifactual ChIP signals.

Stress caused increased binding of p53 to most REs, as expected of the increased stability of p53. However, sites that deviated the most from an RE consensus tended to have low baseline occupancy of p53 and were more highly induced in response to stress. Induced binding to weak sites may be achieved in part through direct or indirect interactions of p53 with other proteins bound to motifs that are positionally constrained with respect to p53 REs. Many REs overlap by 10 bp, whereas others are concentrated at about 250 bp apart. Taken together, these findings paint p53 tetramers as a rather standard DNA binding protein, having structurally stringent DNA binding requirements, and with affinity modulated through variations in DNA sequence. This comes as a surprising conclusion in light of the multiple modes by which p53 has been reported to bind DNA (el-Deiry et al., 1992; Funk et al., 1992; Riley et al., 2008). We attribute the discrepancy to the ability of p53 to bind to degenerate versions of its canonical site that fall below bioinformatic detection but that may have a fortuitous innocuous strong half-site consensus nearby.

RE-Linked Transcription Complexes

We could not definitively link ~90% of all p53-bound REs to a nearby "active" mRNA gene. Yet, most sit very close (<100 bp) to where low levels of TFIIB and Pol II are detected, which we interpret to be transcription initiation complexes. These p53-associated transcription complexes tend to be stress induced but depleted at high levels of p53. Because our data show that p53-bound REs are often embedded within a complex panoply of other stress-regulated transcription factor binding sites, we further conjecture that local noncoding transcription units might be regulated by such factors. Some of these ncRNAs might be functionally important as structural RNAs and, thus, would be expected to be more stable (perhaps polyadenylated and capped) (Djebali et al., 2012). Other RNAs may be irrelevant and degraded as soon as they are made. Instead, the transcription process itself may be important for example to alter the chromatin landscape.

A glimpse at one potential function came with our observation that many of the p53/RE-associated noncoding transcription units reside in an antisense direction to stress-response genes. Critical stress-response genes such as p21, PUMA, and MDM2 appear to have this type of relationship. Just as "futile cycles" exist to simultaneously turn on and off enzymes, offering more dynamic control, production of antisense transcripts may in some cases function to downregulate the expression of the coding sense transcripts. In such cases, like at p21, both sense and antisense may be activated by stress but antagonistic to each other. Regulation of transcription in the antisense direction by p53 may therefore contribute indirectly to the levels of the sense transcripts. p53 may also function directly to activate the sense transcript, perhaps by promoting release of a preassembled paused Pol II; although from this study, we can only conclude that stress causes the release of Pol II into gene bodies. Regardless of the mechanism, the finding that many p53-activated genes are also associated with antisense transcription raises the question as to the extent to which p53 directly controls sense versus antisense transcription.

p53 Permeates the Stress-Response Regulatory Network

Our findings indicate that p53 may directly activate at least 151 annotated genes in U2OS cells in response to UV damage. This number substantially exceeds known direct gene targets of p53. The transcription machinery, as reflected by TFIIB and a paused RNA Pol, is generally preassembled at the promoters of these genes, wherein stress causes the release of paused Pol II into an elongation competent state.

Although p53/RE interactions may regulate local noncoding transcription, most p53/REs could not be linked directly to the regulation of an active gene based on correlated responses to UV treatment. However, those within 15 kb of a TSS or a preassembled initiation complex could be reliably connected and form the basis for a comprehensive p53 regulatory network. Additional p53-regulated genes likely exist but did not meet our experimental criteria for activity and, thus, would be missed. Some may be latent targets that might be picked up in a different cellular state.

In response to various upstream activation signals (e.g., DNA damage), p53 is known to turn on the transcription of distinct sets of target genes, which in turn regulate the cell cycle, cell death, metabolism, and apoptosis (Ma, 2011; Vogelstein et al., 2000; Vousden and Prives, 2009). In agreement with UV irradiation inducing extensive DNA damages, p53 significantly activates the DNA replication, recombination, and repair network genes. Therefore, p53 appears to be an accurate sensor of various cell stresses and appropriately activates the set of genes suitable for the cell's need. Strikingly, this network calls upon p53 target genes involved in all steps of the DNA-damage repair, ranging from halting the cell cycle, regenerating the cellular pools of deoxynucleotide triphosphates, and repairing DNA by both nucleotide excision repair and homologous DNA recombination pathways.

Many feedback loops composed of p53 and its covalent modification enzymes were found, indicating a fine-tuning of the p53 function within this network. In addition, cell death and survival together with metabolism are the top gene networks enriched with p53 target genes after UV irradiation, demonstrating that p53 coordinates multiple pathways in response to a stress. A cell's decision to live or die may be in part regulated by over 100 p53 target genes impinging on interconnected networks. Given the complexity of the p53 network (Vousden and Prives, 2009), future challenges lie with understanding how other signaling cascades and stress-response transcription factors impinge upon p53 regulation. The findings here and elsewhere hint at possible roles for factors that recognize binding sites for the AP1, GATA1, NRF2, FOXO3, and ETS/SPI1 family of transcription factors, as well as stem cell maintenance factors in modulating p53 activity via a direct physical relationship with p53 bound at an RE.

EXPERIMENTAL PROCEDURES

Cell Culture and Stress Treatment

U2OS and HCT116 cells were grown under standard conditions and treated with one of the following stresses: 50 J/m^2 of UV irradiation then cultured for 6 hr, 10 μM nutlin-3a for 6 hr, 1.6 μM doxorubicin for 6 hr, or 350 μM 5-fluorouracil for 6 hr. See also Supplemental Experimental Procedures.

ChIP-Exo

ChIP-exo experiments were carried out essentially as described with minor alterations (Rhee and Pugh, 2012). RNA-seq was carried out on polyA+ selected RNA. Sequencing was performed using Applied Biosystems SOLiD (for p53) and Illumina HiSeq 2000 (for p53, TFIIB, Pol II, and RNA). Uniquely aligned tags were retained and filtered to remove those from heterochromatin and so-called black-listed regions (provided by the ENCODE project).

Data Analysis

See Supplemental Experimental Procedures for additional details and rationale. The set of p53-occupied regions was defined as genomic intervals that lacked a >60 bp gap of tags, and also had a reproducible peak pair as defined in detail in the Supplemental Experimental Procedures. We searched for half-site candidates (consensus RRRC$_4$WWG$_7$YYY) by allowing up to three mismatches, except at the C$_4$ or the G$_7$ position, from 1,824 p53-occupied regions identified in the merged UV-treated (0 and 6 hr) data set from U2OS cells. Next, a search for a second half-site was performed but requiring that any found half-site be 9–22 bp away (midpoint to midpoint, or −1 to 13 bp indel between the half-sites), as justified by the literature. The second half-site was allowed to include one mismatch at either the C$_4$ or the G$_7$ position, but not at both. The total number of mismatches in the two half-sites (or full sites) could not exceed seven. The reason that we chose seven as the limit is that the number of new RE instances fell to near zero at this limit. Only 19 of the top 1,000 occupied regions were at this limit (see Table S1). Only paired half-sites that had at least one half-site with a reproducible tag count greater than zero on each strand in the templated region (described under "Occupancy Determination" in the Supplemental Experimental Procedures) were called as p53 bound.

All potential candidates were screened over a 50 bp range centered to the peak midpoint. Unsplit sites were chosen first in the bound region. If more than one was found in a region, then the most highly occupied sites (up to three) were chosen. Of these, the site with the strongest consensus was chosen (Table S1; Figure 1A). If no unsplit site was found using the above criteria, we then searched for split sites, giving priority to those with the shortest insert. A total of 1,824 regions were grouped preliminarily into group 1P (n = 1,452) and group 2P (n = 265), with the latter containing only those with −1 and 1–13 bp indels. Another 107 regions did not meet the RE criteria and were designated as group 3. This preliminary group 1P set (n = 1,452) was used in the binding sequence analysis shown in Figures 2A, 2B, S2A, and S2B.

Because an unsplit RE (i.e., two half-sites with no insertion) was the most predominant species, and that the degeneracy of an RE might allow the same motif to simultaneously appear as a split and an unsplit motif, we opted for a second sweep through the initial group 2 set using MEME to identify any overrepresented motif. An unsplit RE was returned ($E = 1.6 \times 10^{-97}$). We then applied this group 2 RE position-specific scoring matrix and FIMO ($p < 10^{-3}$) to group 2 and found 119 instances of unsplit REs. These were transferred to group 1P (bottom set of Group 1 in Figure 1A) to make the final group 1 set of 1,571 locations (U2OS, 0 and 6 hr UV) used in parts of this study. The remaining 146 group 2 were subsequently analyzed in Figure S1C. Once convinced that the full sites with ±1 bp indels may be valid REs, we subsequently transferred them to group 1 as part of Table S1 (although were kept as part of group 2 in Figure 1A).

In addition, p53-bound regions were determined with other stress treatments (nutlin-3a, 5-fluorouracil, and doxorubicin), and the finalized group 1 criteria, described above, were used to identify p53-bound REs in response to these other stresses. These were added to the group 1 list to achieve a final set of 2,183 p53-bound REs in Table S1. If a given p53-bound region had multiple REs bound by p53, only the strongest RE was included in Table S1.

ACCESSION NUMBERS

Raw sequencing data are available at NCBI Sequence Read Archive under accession number SRP041136, which includes p53 ChIP-exo and TFIIB, Pol II ChIP-exo with U2OS and HCT116 in response to UV, 5-FU, doxorubicin, and nutlin, and RNA-seq with U2OS in UV stress response.

SUPPLEMENTAL INFORMATION

Supplemental Information includes Supplemental Experimental Procedures, seven figures, and six tables and can be found with this article online at http://dx.doi.org/10.1016/j.celrep.2014.06.030.

AUTHOR CONTRIBUTIONS

X.A.C. and P.L. prepared the cell material. H.S.R. and K.Y.C.-S. prepared the ChIP-exo libraries. T.M. and X.A.C. prepared the RNA-seq libraries. K.H.H. sequenced the libraries. Y.L. and B.F.P. mapped the data. G.S.C. compiled

data and performed integrative genomic analyses. X.A.C. performed and analyzed all other molecular biology experiments. R.C.H. oversaw initial RNA-seq library construction. G.S.C., X.A.C., Y.W., and B.F.P. wrote the paper. B.F.P. oversaw the project.

ACKNOWLEDGMENTS

We thank Joachin Espinosa for compiled lists of p53 target genes and for comments on the manuscript. This work was supported by NIH grants DK065806 (to R.C.H.), CA136856 (to Y.W.), and ES013768 (to B.F.P.). B.F.P. has a financial interest in Peconic, LLC, which utilizes the ChIP-exo technology implemented in this study and could potentially benefit from the outcomes of this research.

Received: April 7, 2014
Revised: May 22, 2014
Accepted: June 18, 2014
Published: July 17, 2014

REFERENCES

Arias-Lopez, C., Lazaro-Trueba, I., Kerr, P., Lord, C.J., Dexter, T., Iravani, M., Ashworth, A., and Silva, A. (2006). p53 modulates homologous recombination by transcriptional regulation of the RAD51 gene. EMBO Rep. *7*, 219–224.

Bandele, O.J., Wang, X., Campbell, M.R., Pittman, G.S., and Bell, D.A. (2011). Human single-nucleotide polymorphisms alter p53 sequence-specific binding at gene regulatory elements. Nucleic Acids Res. *39*, 178–189.

Barsotti, A.M., and Prives, C. (2010). Noncoding RNAs: the missing "linc" in p53-mediated repression. Cell *142*, 358–360.

Bendjennat, M., Boulaire, J., Jascur, T., Brickner, H., Barbier, V., Sarasin, A., Fotedar, A., and Fotedar, R. (2003). UV irradiation triggers ubiquitin-dependent degradation of p21(WAF1) to promote DNA repair. Cell *114*, 599–610.

Botcheva, K., McCorkle, S.R., McCombie, W.R., Dunn, J.J., and Anderson, C.W. (2011). Distinct p53 genomic binding patterns in normal and cancer-derived human cells. Cell Cycle *10*, 4237–4249.

Cawley, S., Bekiranov, S., Ng, H.H., Kapranov, P., Sekinger, E.A., Kampa, D., Piccolboni, A., Sementchenko, V., Cheng, J., Williams, A.J., et al. (2004). Unbiased mapping of transcription factor binding sites along human chromosomes 21 and 22 points to widespread regulation of noncoding RNAs. Cell *116*, 499–509.

Ceribelli, M., Alcalay, M., Viganò, M.A., and Mantovani, R. (2006). Repression of new p53 targets revealed by ChIP on chip experiments. Cell Cycle *5*, 1102–1110.

Cohen, C.J., Lock, W.M., and Mager, D.L. (2009). Endogenous retroviral LTRs as promoters for human genes: a critical assessment. Gene *448*, 105–114.

Djebali, S., Davis, C.A., Merkel, A., Dobin, A., Lassmann, T., Mortazavi, A., Tanzer, A., Lagarde, J., Lin, W., Schlesinger, F., et al. (2012). Landscape of transcription in human cells. Nature *489*, 101–108.

Donehower, L.A., and Bradley, A. (1993). The tumor suppressor p53. Biochim. Biophys. Acta *1155*, 181–205.

el-Deiry, W.S., Kern, S.E., Pietenpol, J.A., Kinzler, K.W., and Vogelstein, B. (1992). Definition of a consensus binding site for p53. Nat. Genet. *1*, 45–49.

Espinosa, J.M., Verdun, R.E., and Emerson, B.M. (2003). p53 functions through stress- and promoter-specific recruitment of transcription initiation components before and after DNA damage. Mol. Cell *12*, 1015–1027.

Freed-Pastor, W.A., and Prives, C. (2012). Mutant p53: one name, many proteins. Genes Dev. *26*, 1268–1286.

Funk, W.D., Pak, D.T., Karas, R.H., Wright, W.E., and Shay, J.W. (1992). A transcriptionally active DNA-binding site for human p53 protein complexes. Mol. Cell. Biol. *12*, 2866–2871.

Gomes, N.P., Bjerke, G., Llorente, B., Szostek, S.A., Emerson, B.M., and Espinosa, J.M. (2006). Gene-specific requirement for P-TEFb activity and RNA polymerase II phosphorylation within the p53 transcriptional program. Genes Dev. *20*, 601–612.

Huarte, M., Guttman, M., Feldser, D., Garber, M., Koziol, M.J., Kenzelmann-Broz, D., Khalil, A.M., Zuk, O., Amit, I., Rabani, M., et al. (2010). A large intergenic noncoding RNA induced by p53 mediates global gene repression in the p53 response. Cell *142*, 409–419.

Jordan, J.J., Menendez, D., Inga, A., Noureddine, M., Bell, D.A., and Resnick, M.A. (2008). Noncanonical DNA motifs as transactivation targets by wild type and mutant p53. PLoS Genet. *4*, e1000104.

Kaeser, M.D., and Iggo, R.D. (2002). Chromatin immunoprecipitation analysis fails to support the latency model for regulation of p53 DNA binding activity in vivo. Proc. Natl. Acad. Sci. USA *99*, 95–100.

Kim, T.K., Hemberg, M., Gray, J.M., Costa, A.M., Bear, D.M., Wu, J., Harmin, D.A., Laptewicz, M., Barbara-Haley, K., Kuersten, S., et al. (2010). Widespread transcription at neuronal activity-regulated enhancers. Nature *465*, 182–187.

Kitayner, M., Rozenberg, H., Kessler, N., Rabinovich, D., Shaulov, L., Haran, T.E., and Shakked, Z. (2006). Structural basis of DNA recognition by p53 tetramers. Mol. Cell *22*, 741–753.

Kurokawa, M., Kim, J., Geradts, J., Matsuura, K., Liu, L., Ran, X., Xia, W., Ribar, T.J., Henao, R., Dewhirst, M.W., et al. (2013). A network of substrates of the E3 ubiquitin ligases MDM2 and HUWE1 control apoptosis independently of p53. Sci. Signal. *6*, ra32.

Laptenko, O., and Prives, C. (2006). Transcriptional regulation by p53: one protein, many possibilities. Cell Death Differ. *13*, 951–961.

Lew, Q.J., Chia, Y.L., Chu, K.L., Lam, Y.T., Gurumurthy, M., Xu, S., Lam, K.P., Cheong, N., and Chao, S.H. (2012). Identification of HEXIM1 as a positive regulator of p53. J. Biol. Chem. *287*, 36443–36454.

Lidor Nili, E., Field, Y., Lubling, Y., Widom, J., Oren, M., and Segal, E. (2010). p53 binds preferentially to genomic regions with high DNA-encoded nucleosome occupancy. Genome Res. *20*, 1361–1368.

Liu, G., and Chen, X. (2006). DNA polymerase eta, the product of the xeroderma pigmentosum variant gene and a target of p53, modulates the DNA damage checkpoint and p53 activation. Mol. Cell. Biol. *26*, 1398–1413.

Lockwood, W.W., Zejnullahu, K., Bradner, J.E., and Varmus, H. (2012). Sensitivity of human lung adenocarcinoma cell lines to targeted inhibition of BET epigenetic signaling proteins. Proc. Natl. Acad. Sci. USA *109*, 19408–19413.

Loeb, L.A., and Monnat, R.J., Jr. (2008). DNA polymerases and human disease. Nat. Rev. Genet. *9*, 594–604.

Ma, J. (2011). Transcriptional activators and activation mechanisms. Protein & cell *2*, 879–888.

Marín-Béjar, O., Marchese, F.P., Athie, A., Sánchez, Y., González, J., Segura, V., Huang, L., Moreno, I., Navarro, A., Monzó, M., et al. (2013). Pint lincRNA connects the p53 pathway with epigenetic silencing by the Polycomb repressive complex 2. Genome Biol. *14*, R104.

Masutani, C., Kusumoto, R., Yamada, A., Dohmae, N., Yokoi, M., Yuasa, M., Araki, M., Iwai, S., Takio, K., and Hanaoka, F. (1999). The XPV (xeroderma pigmentosum variant) gene encodes human DNA polymerase eta. Nature *399*, 700–704.

McLure, K.G., and Lee, P.W. (1998). How p53 binds DNA as a tetramer. EMBO J. *17*, 3342–3350.

Melo, C.A., Drost, J., Wijchers, P.J., van de Werken, H., de Wit, E., Oude Vrielink, J.A., Elkon, R., Melo, S.A., Léveillé, N., Kalluri, R., et al. (2013). eRNAs are required for p53-dependent enhancer activity and gene transcription. Mol. Cell *49*, 524–535.

Menendez, D., Inga, A., and Resnick, M.A. (2009). The expanding universe of p53 targets. Nat. Rev. Cancer *9*, 724–737.

Menendez, D., Nguyen, T.A., Freudenberg, J.M., Mathew, V.J., Anderson, C.W., Jothi, R., and Resnick, M.A. (2013). Diverse stresses dramatically alter genome-wide p53 binding and transactivation landscape in human cancer cells. Nucleic Acids Res. *41*, 7286–7301.

Morozova, O., Hirst, M., and Marra, M.A. (2009). Applications of new sequencing technologies for transcriptome analysis. Annu. Rev. Genomics Hum. Genet. *10*, 135–151.

Naqvi, A., Hoffman, T.A., DeRicco, J., Kumar, A., Kim, C.S., Jung, S.B., Yamamori, T., Kim, Y.R., Mehdi, F., Kumar, S., et al. (2010). A single-nucleotide variation in a p53-binding site affects nutrient-sensitive human SIRT1 expression. Hum. Mol. Genet. *19*, 4123–4133.

Nikulenkov, F., Spinnler, C., Li, H., Tonelli, C., Shi, Y., Turunen, M., Kivioja, T., Ignatiev, I., Kel, A., Taipale, J., and Selivanova, G. (2012). Insights into p53 transcriptional function via genome-wide chromatin occupancy and gene expression analysis. Cell Death Differ. *19*, 1992–2002.

Ørom, U.A., and Shiekhattar, R. (2013). Long noncoding RNAs usher in a new era in the biology of enhancers. Cell *154*, 1190–1193.

Ptashne, M., and Gann, A. (1997). Transcriptional activation by recruitment. Nature *386*, 569–577.

Qian, H., Wang, T., Naumovski, L., Lopez, C.D., and Brachmann, R.K. (2002). Groups of p53 target genes involved in specific p53 downstream effects cluster into different classes of DNA binding sites. Oncogene *21*, 7901–7911.

Rahl, P.B., Lin, C.Y., Seila, A.C., Flynn, R.A., McCuine, S., Burge, C.B., Sharp, P.A., and Young, R.A. (2010). c-Myc regulates transcriptional pause release. Cell *141*, 432–445.

Renault, V.M., Thekkat, P.U., Hoang, K.L., White, J.L., Brady, C.A., Kenzelmann Broz, D., Venturelli, O.S., Johnson, T.M., Oskoui, P.R., Xuan, Z., et al. (2011). The pro-longevity gene FoxO3 is a direct target of the p53 tumor suppressor. Oncogene *30*, 3207–3221.

Rhee, H.S., and Pugh, B.F. (2011). Comprehensive genome-wide protein-DNA interactions detected at single-nucleotide resolution. Cell *147*, 1408–1419.

Rhee, H.S., and Pugh, B.F. (2012). ChIP-exo method for identifying Genomic location of DNA-binding proteins with near-single-nucleotide accuracy. Curr. Protoc. Mol. Biol. *Chapter 21*, Unit21 24.

Riley, T., Sontag, E., Chen, P., and Levine, A. (2008). Transcriptional control of human p53-regulated genes. Nat. Rev. Mol. Cell Biol. *9*, 402–412.

Rotblat, B., Melino, G., and Knight, R.A. (2012). NRF2 and p53: Januses in cancer? Oncotarget *3*, 1272–1283.

Rougvie, A.E., and Lis, J.T. (1988). The RNA polymerase II molecule at the 5′ end of the uninduced hsp70 gene of D. melanogaster is transcriptionally engaged. Cell *54*, 795–804.

Schlereth, K., Heyl, C., Krampitz, A.M., Mernberger, M., Finkernagel, F., Scharfe, M., Jarek, M., Leich, E., Rosenwald, A., and Stiewe, T. (2013). Characterization of the p53 cistrome—DNA binding cooperativity dissects p53's tumor suppressor functions. PLoS Genet. *9*, e1003726.

Shaked, H., Shiff, I., Kott-Gutkowski, M., Siegfried, Z., Haupt, Y., and Simon, I. (2008). Chromatin immunoprecipitation-on-chip reveals stress-dependent p53 occupancy in primary normal cells but not in established cell lines. Cancer Res. *68*, 9671–9677.

Sherry, S.T., Ward, M.H., Kholodov, M., Baker, J., Phan, L., Smigielski, E.M., and Sirotkin, K. (2001). dbSNP: the NCBI database of genetic variation. Nucleic Acids Res. *29*, 308–311.

Shinobu, N., Maeda, T., Aso, T., Ito, T., Kondo, T., Koike, K., and Hatakeyama, M. (1999). Physical interaction and functional antagonism between the RNA polymerase II elongation factor ELL and p53. J. Biol. Chem. *274*, 17003–17010.

Smeenk, L., van Heeringen, S.J., Koeppel, M., van Driel, M.A., Bartels, S.J., Akkers, R.C., Denissov, S., Stunnenberg, H.G., and Lohrum, M. (2008). Characterization of genome-wide p53-binding sites upon stress response. Nucleic Acids Res. *36*, 3639–3654.

Smeenk, L., van Heeringen, S.J., Koeppel, M., Gilbert, B., Janssen-Megens, E., Stunnenberg, H.G., and Lohrum, M. (2011). Role of p53 serine 46 in p53 target gene regulation. PLoS One *6*, e17574.

Thut, C.J., Chen, J.L., Klemm, R., and Tjian, R. (1995). p53 transcriptional activation mediated by coactivators TAFII40 and TAFII60. Science *267*, 100–104.

Tidow, H., Melero, R., Mylonas, E., Freund, S.M., Grossmann, J.G., Carazo, J.M., Svergun, D.I., Valle, M., and Fersht, A.R. (2007). Quaternary structures of tumor suppressor p53 and a specific p53 DNA complex. Proc. Natl. Acad. Sci. USA *104*, 12324–12329.

Tu, S.P., Chi, A.L., Ai, W., Takaishi, S., Dubeykovskaya, Z., Quante, M., Fox, J.G., and Wang, T.C. (2009). p53 inhibition of AP1-dependent TFF2 expression induces apoptosis and inhibits cell migration in gastric cancer cells. Am. J. Physiol. Gastrointest. Liver Physiol. *297*, G385–G396.

Valentine, J.M., Kumar, S., and Moumen, A. (2011). A p53-independent role for the MDM2 antagonist Nutlin-3 in DNA damage response initiation. BMC Cancer *11*, 79.

Vogelstein, B., and Kinzler, K.W. (1992). p53 function and dysfunction. Cell *70*, 523–526.

Vogelstein, B., Lane, D., and Levine, A.J. (2000). Surfing the p53 network. Nature *408*, 307–310.

Vousden, K.H., and Prives, C. (2009). Blinded by the light: the growing complexity of p53. Cell *137*, 413–431.

Wang, B., Niu, D., Lam, T.H., Xiao, Z., and Ren, E.C. (2014). Mapping the p53 transcriptome universe using p53 natural polymorphs. Cell Death Differ. *21*, 521–532.

Wei, C.L., Wu, Q., Vega, V.B., Chiu, K.P., Ng, P., Zhang, T., Shahab, A., Yong, H.C., Fu, Y., Weng, Z., et al. (2006). A global map of p53 transcription-factor binding sites in the human genome. Cell *124*, 207–219.

Yu, J., Zhang, L., Hwang, P.M., Rago, C., Kinzler, K.W., and Vogelstein, B. (1999). Identification and classification of p53-regulated genes. Proc. Natl. Acad. Sci. USA *96*, 14517–14522.

Zhao, R., Gish, K., Murphy, M., Yin, Y., Notterman, D., Hoffman, W.H., Tom, E., Mack, D.H., and Levine, A.J. (2000). Analysis of p53-regulated gene expression patterns using oligonucleotide arrays. Genes Dev. *14*, 981–993.

Zhou, B., Westaway, S.K., Levinson, B., Johnson, M.A., Gitschier, J., and Hayflick, S.J. (2001). A novel pantothenate kinase gene (PANK2) is defective in Hallervorden-Spatz syndrome. Nat. Genet. *28*, 345–349.

Zhu, N., Gu, L., Findley, H.W., Chen, C., Dong, J.T., Yang, L., and Zhou, M. (2006). KLF5 Interacts with p53 in regulating survivin expression in acute lymphoblastic leukemia. J. Biol. Chem. *281*, 14711–14718.